Towards Accurate Partial Volume Correction – Perturbation for SPECT Resolution Estimation

Rebecca Gillen, *Student Member, IEEE*, Kjell Erlandsson, Ana M Denis-Bacelar, Kris Thielemans *Senior Member, IEEE*, Brian F Hutton, *Senior Member, IEEE*, Sarah McQuaid

***Abstract*–The accuracy of quantitative SPECT imaging is limited by the Partial Volume Effect as a result of the relatively poor spatial resolution. There is currently no consensus on the optimal Partial Volume Correction (PVC) algorithm in the application of SPECT oncology imaging. Several promising candidates require information on the reconstructed resolution - usually in the form of the Point Spread Function (PSF). A particular challenge that SPECT poses for PVC is that the resolution is known to vary with position in the field-of-view, as well as with activity distribution and reconstruction method. In this work, we assessed the potential benefit of using perturbation to measure case-specific resolution for PVC. A small point source was used to measure the resolution in phantoms designed to replicate the issues encountered in oncology imaging, including anthropomorphic phantoms which had not previously been examined in perturbation applications. Results demonstrate that, provided that a sufficient number of iterations is used for image reconstruction, perturbation can be used to measure a case-specific PSF. When PVC is applied with this case-specific PSF, quantitative accuracy is improved compared with no correction or applying PVC with an inappropriate PSF.**

I. Introduction

THE Partial Volume Effect (PVE) leads to quantitative inaccuracies in the measurement of activity concentration of small objects. In oncology imaging, this may impact diagnosis, dosimetry, and monitoring treatment response.

Several Partial Volume Correction (PVC) algorithms have been proposed in the literature [1], but there is currently no consensus on which method to use in oncology. The Point Spread Function (PSF) is known to depend on factors including activity distribution, reconstruction method and, particularly for SPECT imaging, the position in the Field-of-View (FOV). Several PVC methods require information on the reconstructed resolution, and so a case-specific measure of PSF is required for accurate application of PVC in oncology SPECT.

Perturbation, by the addition of a small source to projection data, has previously been shown to be effective for estimating the local reconstructed PSF in simple phantoms [2]–[4]. However, perturbation has not yet been tested with oncology SPECT as the main application. Specific challenges raised by oncology imaging include variability in sizes, shapes, and lesion intensities (in contrast to the relatively predictable anatomy of neuro and cardiac imaging). In addition, the benefits of applying PVC with a local, case-specific PSF, as estimated by perturbation, have not yet been demonstrated.

The aim of this work was to assess the potential benefit of applying PVC using a case-specific resolution estimated using perturbation in oncology SPECT imaging.

II. Methods

Phantoms of activity distribution and attenuation were generated and reconstructed with STIR [5], simulating SPECT ^{99m}Tc imaging using parameters representing a Mediso Anyscan Trio system with LEHR collimators. Noise-free and noisy datasets were generated.

A. Phantom Generation

An elliptical cylinder with axes of 304 × 216 mm and length 216 mm was generated on a 128 × 128 matrix with 4 mm^3 voxels. To this uniform elliptical background, uniform spheres of different radii and target to background ratios (TBRs) were added at the centre of the FOV, and at a position 8 cm off-centre. These phantom data were forward projected using a circular orbit with radius of rotation = 26 cm.

An anthropomorphic dataset was also used. XCAT phantom [6] data, representing a ^{99m}Tc phosphate scan for bone imaging, were generated on a 256 × 256 matrix with 2.2mm^3 voxels. A uniform 15 mm diameter lesion was positioned in the pelvis and assigned intensity such that the target to background ratio (lesion to normal bone) was 5:1. Data were forward projected based on an elliptical orbit and sinograms were generated on a 128 × 128 matrix with 4.4mm^3 voxels.

Representative example image slices showing the simple and anthropomorphic phantoms are included in Fig. 1.

Manuscript received November 29, 2021. RG is completing a PhD with funding from the Industrial Strategy Challenge Fund via NPL - supported by the National Measurement System of the UK Department for Business, Energy, and Industrial Strategy. Staff at the Institute of Nuclear Medicine receive support from the NIHR University College London Hospitals Biomedical Research Centre. AMDB is supported by the National Measurement System of the UK Department for Business, Energy, and Industrial Strategy. The Open Source software STIR is supported by EPSRC grant EP/T026693/1.

R. Gillen is with the Institute of Nuclear Medicine, University College London, UK (e-mail: Rebecca.Gillen.18@ucl.ac.uk).

S. McQuaid is with the Institute of Nuclear Medicine, University College London, UK (e-mail: Sarah.McQuaid@nhs.net).

K. Thielemans is with the Institute of Nuclear Medicine, University College London, UK (e-mail: k.thielemans@ucl.ac.uk).

B. F. Hutton is with the Institute of Nuclear Medicine, University College London, UK (e-mail: b.hutton@ucl.ac.uk).

K. Erlandsson is with the Institute of Nuclear Medicine, University College London, UK (e-mail: k.erlandsson@ucl.ac.uk).

A. M. Denis-Bacelar is with the National Physical Laboratory, Teddington, UK (email: ana.denisbacelar@npl.co.uk).

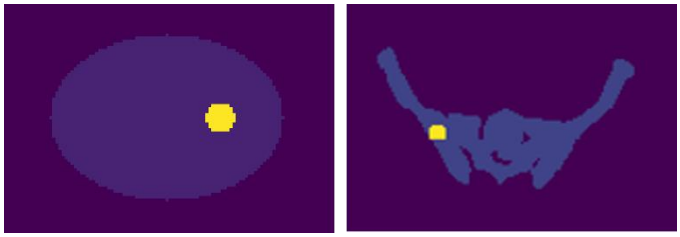

Fig. 1. Images showing representative slices of phantoms used in this investigation. On the left, an example of the simple geometrical phantom with a spherical lesion. On the right an example of an anthropomorphic phantom, including 15 mm diameter pelvic lesion, created using XCAT data.

B. Perturbation, Reconstruction and Analysis

Projections of low intensity, single voxel, point sources were added to the forward projections of the phantoms. Point source intensity relative to the surrounding background was set in line with previous work on perturbation [4]. Reconstructions were performed using OSEM, up to 20 iterations with 10 subsets. Images were saved every 10 updates (i.e. every full iteration). Reconstructed images of phantoms were subtracted from reconstructions with the added point sources, producing an image of the PSF at the position of each point source. Assuming an anisotropic 3D Gaussian PSF, 2D Gaussians were fitted in each orthogonal plane to determine the Full Width at Half Maximum (FWHM) in each direction.

PVC using the Single Target Correction (STC) method [7] was applied to the lesions in the simple and anthropomorphic phantoms. Post-correction regional mean values (RMVs) within the lesions were then calculated.

III. Results

FWHM measurements in each direction were found to vary with reconstruction update number. This is demonstrated in Fig. 2 for a point centered on a 36 mm radius lesion in the simple elliptical phantom with TBR = 10, positioned 8 cm from the centre of the FOV. This dependence implies that a perturbation-based PSF should not be used to apply PVC on images reconstructed using different parameters to those which were used for the PSF measurement, even if the same raw data are used.

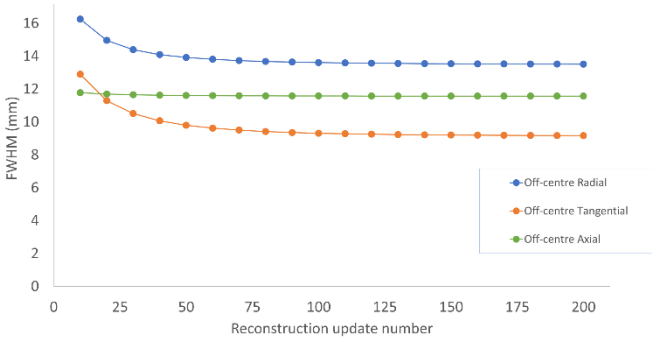

Fig. 2. Plot of perturbation-measured FWHM values in each direction vs OSEM update number (where 200 updates is 20 iterations with 10 subsets). These data were measured in the simple elliptical phantom, for a point 8 cm from the centre of the FOV, centered on a 36 mm radius lesion, with TBR =10.

The measured PSF was dependent on the position in the FOV. Fig. 2 shows that, by 200 updates, the estimated PSF is anisotropic, with different values in each direction for a point positioned away from the centre of the FOV. This is an expected result, consistent with known positional variation in SPECT imaging. Fig. 3 compares FWHM values measured in images reconstructed with 200 updates for an off-centre point and a central point. For the central point, FWHM measurements demonstrate an approximately isotropic PSF. The assumption of an isotropic, invariant PSF for SPECT imaging is inappropriate in off-centre positions, and may impact on quantification if used for PVC.

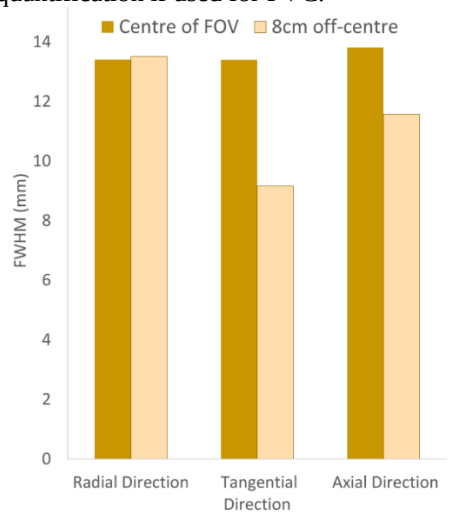

Fig. 3. Comparison of FWHM values in each direction for two different positions in the FOV for simple elliptical phantom data – the centre of the FOV and 8 cm off-centre at 200 OSEM updates. The central PSF is approximately isotropic (each direction was within 3% of 13.4 mm). The off-centre PSF is comparatively anisotropic.

FWHM measurements were found to depend on the lesion TBR at low reconstruction updates. Fig. 4 demonstrates this in the tangential direction for 36 mm lesions positioned centrally in the FOV and also 8 cm off-centre. Fig. 4 also shows that this dependence reduces with increasing reconstruction updates, and the measured FWHM values are approximately independent of TBR by 100 reconstruction updates.

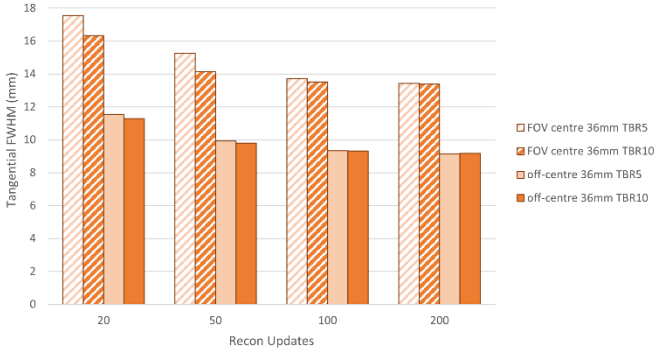

Fig. 4. FWHM values in the tangential direction vs OSEM update number for the simple elliptical phantom, with a point centered on a 36 mm radius lesion, and the lesion positioned either at the centre of the FOV or 8cm off-centre, and where the TBR was either 5 or 10. This demonstrates that the FWHM measurement depended on TBR at low reconstruction updates, but this dependence reduced with more reconstruction updates.

Dependence on lesion contrast may be important when serial measurements are made – for example monitoring treatment response, since tracer avidity may change. However, reconstructing with a sufficient number of iterations could help to ensure consistent PSF measurement and therefore a consistent application of PVC (note that this may be more iterations than used in routine clinical practice).

Adding Poisson noise to projections of the simple geometric phantom data did not affect the measured PSF - any differences were within the uncertainties of the Gaussian fitting.

Perturbation-measured FWHM results were also produced for the XCAT dataset. Variations in surrounding activity was not found to impact the FWHM – setting up the phantom with a full and empty bladder resulted in negligible difference above 30 updates. This, again, supports the recommendation to use a sufficient number of updates to reduce the variability in PSF measurement. The number of updates required to reach an approximately steady value were found to be lower for the XCAT data than the ellipse (ellipse data took approximately 100 updates, as seen in Fig.2) which may be due to the sparser surrounding activity distribution.

PVC with STC using perturbation-based PSF measurements improved image appearance, as shown for XCAT data in Fig. 5. In particular, the edges of the segmented regions are better defined. This may be helpful in visual lesion detection, provided that segmentation is performed accurately.

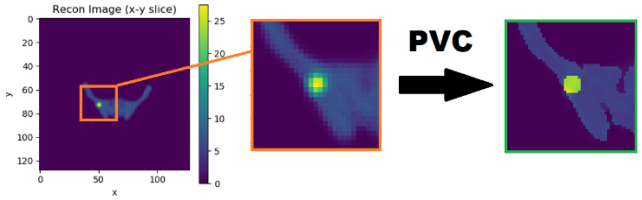

Fig. 5. Reconstructed XCAT data highlighting the local region of interest, demonstrating the loss of resolution in the uncorrected image. After PVC using the local case-specific PSF measured by perturbation, edge definition is improved.

Quantitative accuracy, in terms of the RMV was improved when PVC was applied with the perturbation-based PSF, compared with uncorrected data. PVC with perturbation-based PSF was also found to be quantitatively superior to PVC applied with a PSF measured at the centre of the FOV (i.e. a non-case-specific resolution, but one which may be assumed in the absence of other measurements). RMV results for the pelvis lesion are shown in Fig. 6, with a ground truth value of 36. The uncorrected image underestimated the RMV by 47%, correcting with PVC using the perturbation-specific PSF resulted in a RMV 11% lower than the ground truth. However, correcting with PVC using a PSF measured at the centre of the FOV resulted in an overestimation of the lesion RMV by 51%. While an 11% discrepancy leaves some room for improvement in the PVC process, it is an improvement in accuracy compared with the other options of no correction or correction with an inappropriate PSF. These other options may result in inaccurate assessment of lesion uptake and could potentially impact patient management.

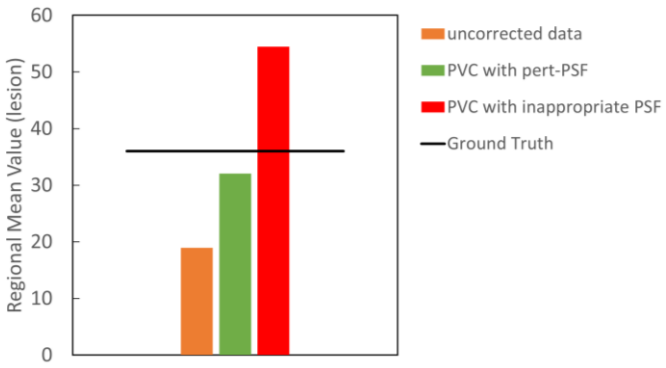

Fig. 6. Regional mean values for a 15 mm diameter pelvic lesion (contrast 5:1) for uncorrected images, images corrected by STC using a perturbation-measured PSF, and images corrected by STC using a PSF measured at the centre of the FOV for images reconstructed with 200 updates.

Ten STC iterations was found to be sufficient, as seen in previous work [4]. However, further work is required to optimize the implementation of STC with perturbation, and/or other PVC algorithms, in the application of oncology SPECT.

IV. Conclusions

Perturbation can be used to measure SPECT resolution, and can accurately capture PSF variation with a number of factors relevant to oncology imaging, including position in FOV, provided that a sufficient number of reconstruction updates are used.

Image appearance and quantitative accuracy are improved when PVC is applied with STC using a case-specific PSF compared with no correction, or using an inappropriate PSF.

References

[1] K. Erlandsson, I. Buvat, P. H. Pretorius, B. A. Thomas, and B. F. Hutton, "A review of partial volume correction techniques for emission tomography and their applications in neurology, cardiology and oncology," *Phys. Med. Biol.*, vol. 57, no. 21, pp. R119–R159, Nov. 2012.

[2] J. A. Stamos, W. L. Rogers, N. H. Clinthorne, and K. F. Koral, "Object-dependent performance comparison of two iterative reconstruction algorithms," *IEEE Trans. Nucl. Sci.*, vol. 35, no. 1, pp. 611–614, 1988.

[3] J.S. Liow and S. C. Strother, "The convergence of object dependent resolution in maximum likelihood based tomographic image reconstruction," *Phys. Med. Biol.*, vol. 38, no. 1, pp. 55–70, Jan. 1993.

[4] K. Gong, S. R. Cherry, and J. Qi, "On the assessment of spatial resolution of PET systems with iterative image reconstruction," *Phys. Med. Biol.*, vol. 61, no. 5, pp. N193–N202, Feb. 2016.

[5] B. Marti-Fuster *et al.*, "Integration of advanced 3D SPECT modeling into the open-source STIR framework," *Med. Phys.*, vol. 40, no. 9, p. 092502, Aug. 2013.

[6] W. P. Segars, B. M. W. Tsui, J. Cai, F. F. Yin, G. S. K. Fung, and E. Samei, "Application of the 4-D XCAT Phantoms in Biomedical Imaging and beyond," *IEEE Trans. Med. Imaging*, vol. 37, no. 3, pp. 680–692, Mar. 2018.

[7] K. Erlandsson and B. F. Hutton, "A novel voxel-based partial volume correction method for single regions of interest," *J. Nucl. Med.*, vol. 55, no. supplement 1, pp. 2123–2123, May 2014.